Figure S1

A

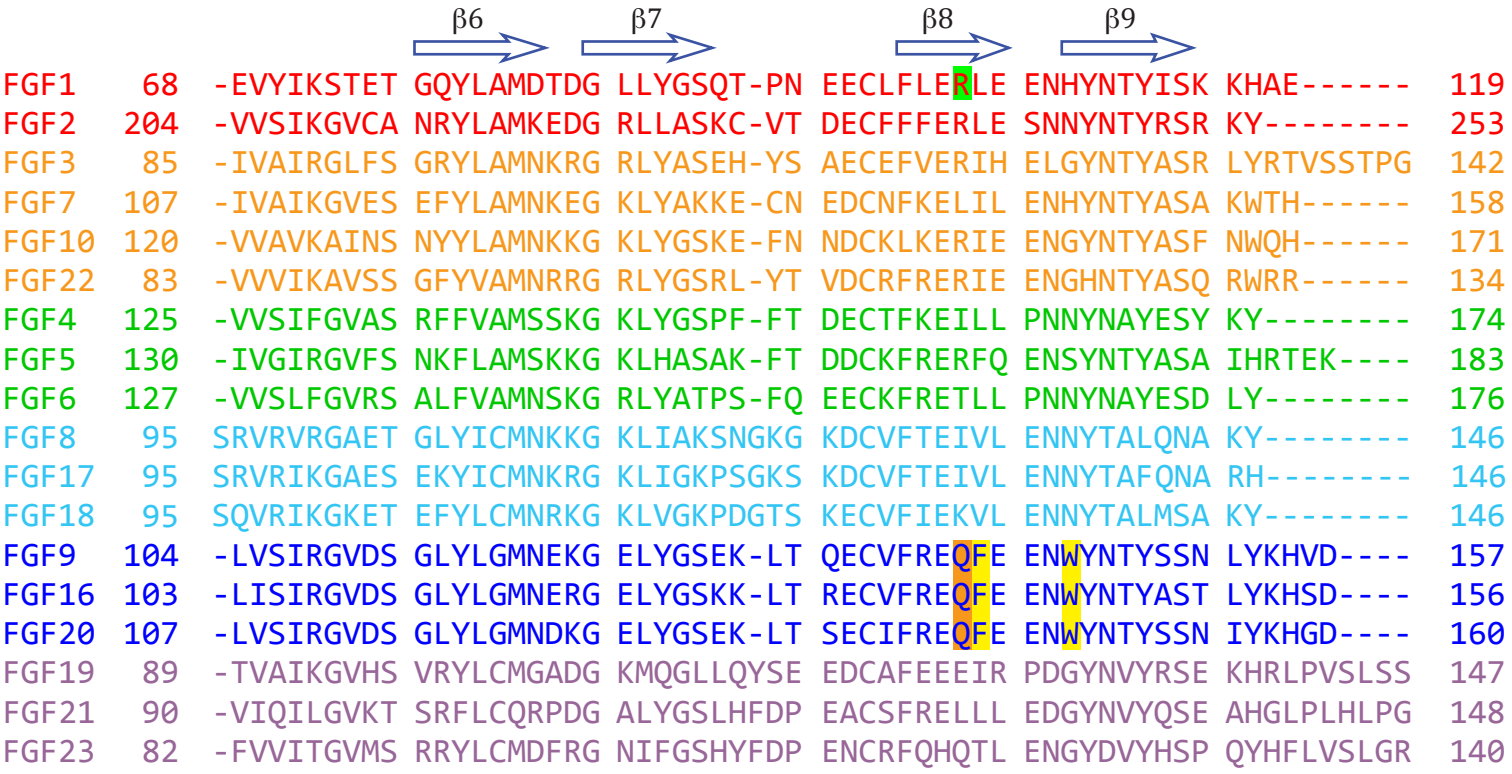

B

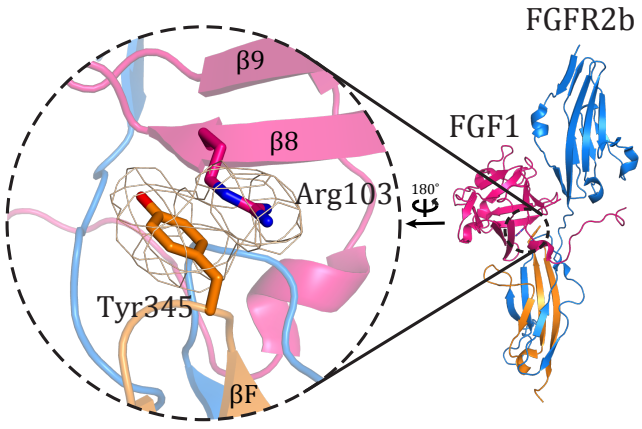

C

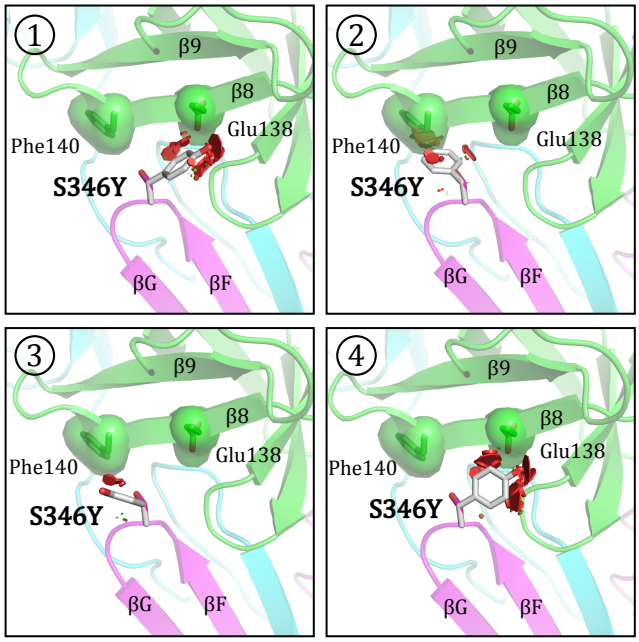

Figure S2

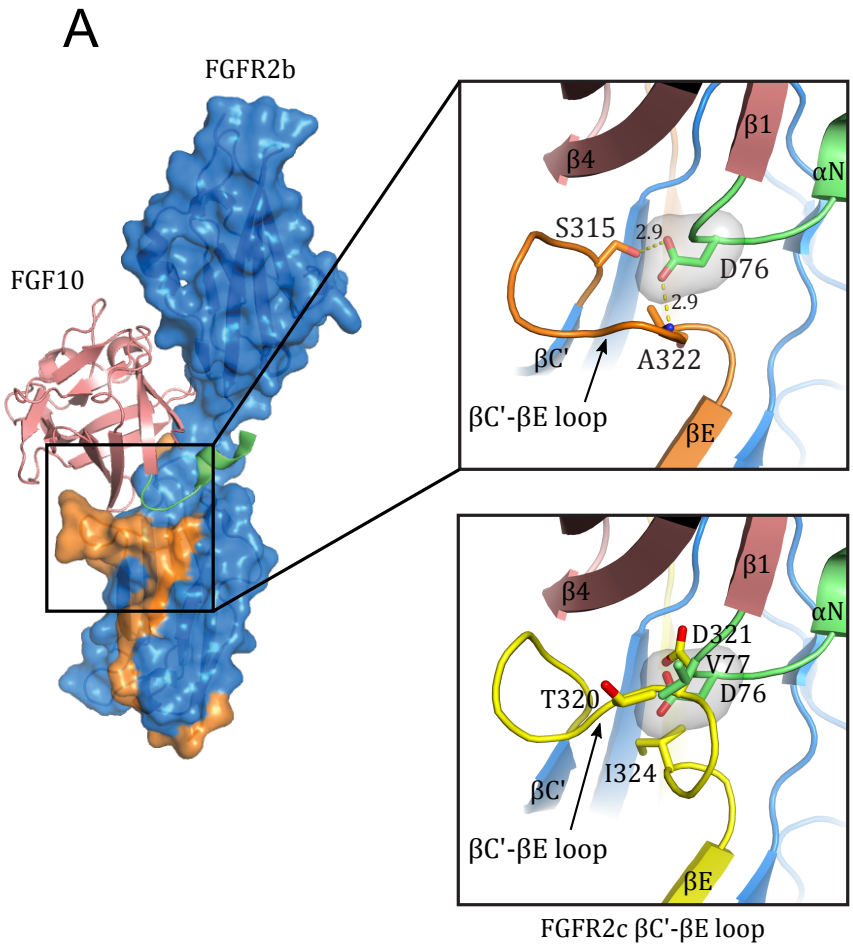

Mode 1

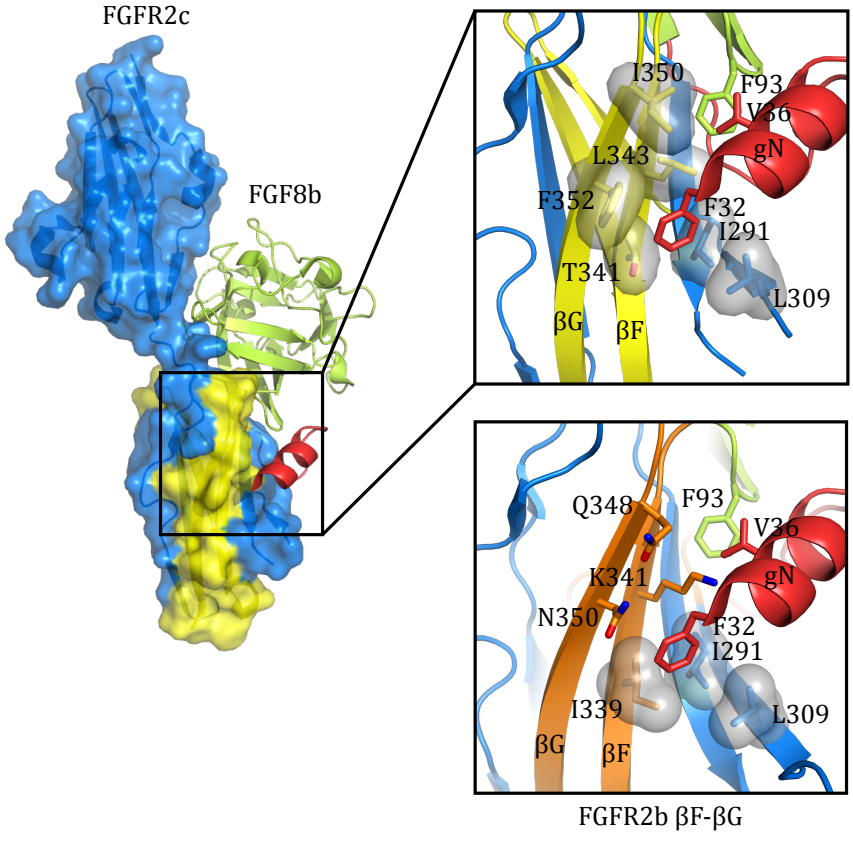

Mode 2

Figure S1. Sequence alignment of FGFs and differential effects of the S346Y mutation in FGFR1c on FGF binding (related to Figure 2, 3, 4, and 6)

(**A**) Sequence alignment of a section of β-trefoil region encompassing β6 to β9 strands of 18 human FGFs. β strands are shown on top of the alignment and labeled according to conventional nomenclature for the FGF β-trefoil fold . The six FGF subfamilies are distinguished with different colors. The first and last residue for each sequence are numbered. The unique Phe and Trp residues in the β8 and β9 strands, respectively, of the FGF9 subfamily that are critical in regulating this subfamily's receptor-binding specificity, are highlighted in yellow. Unique conservation of Gln-139 of FGF9 among FGF9 subfamily ligands is emphasized by orange coloring. In FGF1, Arg-103 (highlighted in green) occupies the position corresponding to this conserved Gln of FGF9 subfamily. (**B**) Cartoon representation of the FGF1-FGFR2b complex structure (PDB ID: 3OJM) . FGF1 is in red, and FGFR2b is colored in blue except for its alternatively spliced region, which is in orange. Close-up view of the interface between FGF1 and the βF-βG loop in FGFR2b D3 showing the π-cation interaction between FGF1 Arg-103 and FGFR2b Tyr-345. This arginine residue is a glutamine in the FGF9 subfamily (highlighted in orange in panel A). This Arg->Gln substitution eliminates the possibility of a π-cation interaction between FGF9 subfamily ligands and the 'b' splice isoform specific tyrosine in the βF-βG loop of FGFR 'b' isoforms. Moreover, a glutamine in this location also introduces a spatial clash with the side chain of the tyrosine further discouraging binding of FGF9 subfamily ligands to FGFR 'b' isoforms. (**C**) A tyrosine at the amino acid position 346 of FGFR1c is incompatible with FGF9 binding as modeled by *PyMOL*. Panels 1 through 4 illustrate that presence of a tyrosine at this location would cause steric clashes and loss of water-mediated hydrogen bond between FGFR1c and FGF9. The mutated tyrosine is shown in white sticks, and clashes between the mutated tyrosine and FGF9 are indicated by red plates.

Figure S2. FGF10-FGFR2b and FGF8b-FGFR2c complex structures showing two distinct modes by which the N-termini of FGF10 and FGF8b dictate FGF-FGFR binding specificity (related to Figure 5)

(**A**) Crystal structure of the FGF10-FGFR2b complex (PDB ID: 1NUN) . Molecular surface of FGFR2b is shown and colored in blue except for its alternatively spliced region, which is in orange. FGF10 is shown as cartoon with its N-terminus and core region colored in dark green and pink, respectively. Upper inset to the right, shows expanded view of the hydrogen bonds between Asp-76 from the FGF10 N-terminus and Ser-315 and Ala-322 in the βC'-βE loop of FGFR2b D3. In the lower box, the FGFR2b D3 domain has been swapped by the corresponding FGFR2c D3 domain. The alternatively spliced region of FGFR2c D3 is colored yellow. Note that both steric and electrostatic clashes between the FGF10 N-terminus and the βC'-βE loop of FGFR2c D3 prevent FGF10 from binding to FGFR2c isoform. (**B**) Crystal structure of the FGF8b-FGFR2c complex (PDB ID: 2FDB) . Relative to the FGF10-FGFR2b complex in panel A, which is shown in a typical "front view", the FGF8b-FGFR2c complex is rotated by 180° around the vertical axis to show the back of the complex. FGF8b is shown in cartoon with its N-terminus and core region colored in red and light green, respectively. Molecular surface of FGFR2c is colored in blue except for its alternatively spliced region in D3 which is in yellow. Top right inset: an expanded view of the boxed region showing the hydrophobic interactions between the FGF8b N-terminus and the hydrophobic groove in FGFR2c D3 that is conserved in "c" splice isoforms of FGFR1-3 and FGFR4. Bottom inset shows that three out of six hydrophobic residues, which interact with the FGF8b N-terminus, are replaced by polar residues in the alternatively spliced region (in orange) of FGFR2b. This explains the inability of FGF8b to bind and activate FGFR2b.